


Article

Nitroxide-Mediated Copolymerization of Itaconate Esters with Styrene

Sepehr Kardan ¹, Omar Garcia Valdez ^{1,2}, Adrien Métafiot ¹ and Milan Maric ^{1,*} 

¹ Department of Chemical Engineering, McGill University, Montreal, QC H3A 0C5, Canada; sepehr.kardan@mail.mcgill.ca (S.K.); ogarciavaldez@greencentrecanada.com (O.G.V.); adrien.metafiot2@mcgill.ca (A.M.)

² Green Center Canada, 945 Princess Street, Suite 105, Kingston, ON K7L 0E9, Canada

* Correspondence: milan.maric@mcgill.ca; Tel.: +1-514-398-4272

Received: 19 March 2019; Accepted: 27 April 2019; Published: 1 May 2019



Abstract: Replacing petro-based materials with renewably sourced ones has clearly been applied to polymers, such as those derived from itaconic acid (IA) and its derivatives. Di-n-butyl itaconate (DBI) was (co)polymerized via nitroxide mediated polymerization (NMP) to impart elastomeric (rubber) properties. Homopolymerization of DBI by NMP was not possible, due to a stable adduct being formed. However, DBI/styrene (S) copolymerization by NMP at various initial molar feed compositions $f_{DBI,0}$ was polymerizable at different reaction temperatures (70–110 °C) in 1,4 dioxane solution. DBI/S copolymerizations largely obeyed first order kinetics for initial DBI compositions of 10% to 80%. Number-average molecular weight (M_n) versus conversion for various DBI/S copolymerizations however showed significant deviations from the theoretical M_n as a result of chain transfer reactions (that are more likely to occur at high temperatures) and/or the poor reactivity of DBI via an NMP mechanism. In order to suppress possible intramolecular chain transfer reactions, the copolymerization was performed at 70 °C and for a longer time (72 h) with $f_{DBI,0} = 50\%$ – 80% , and some slight improvements regarding the dispersity ($\bar{D} = 1.3$ – 1.5), chain activity and conversion ($\sim 50\%$) were observed for the less DBI-rich compositions. The statistical copolymers produced showed a depression in T_g relative to poly(styrene) homopolymer, indicating the effect of DBI incorporation.

Keywords: nitroxide mediated polymerization; itaconate esters; copolymerization

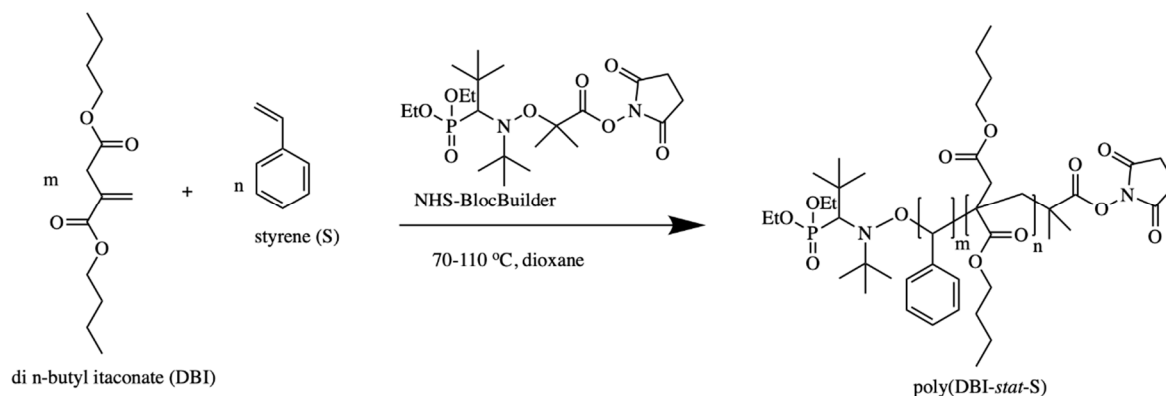
1. Introduction

The limited supply of fossil resources has forced the exploration of renewable feedstocks as an alternative route to materials such as polymers [1]. One such feedstock for polymers is itaconic acid (IA), which was first isolated from the pyrolysis of citric acid [2,3] and is now made by fermentation from fungi [3,4]. IA has been used historically in coatings, adhesives, binders and thickeners [1,5–8]. Itaconic acid's high availability, low cost, structural similarity with acrylates and methacrylates, and its dicarboxylic acid functionality have motivated research on the development of polymeric materials from IA and derivatives like dialkyl itaconates or β monoalkyl itaconates [9,10]. Itaconic acid is indeed listed as one of the most promising bio-based feedstocks according to a report from the Biomass Program of the US Department of Energy [9]. The dual functionality of IA is particularly appealing as it makes it possible to polymerize it via free radical mechanisms (Marvel and Shepherd first described it in 1959 [11]), step-wise polymerization mechanisms (such as using ring-opening step-wise polymerization of itaconic anhydride [12–14]), ring-opening metathesis polymerizations (ROMP) [15,16] and acyclic diene metathesis (ADMET) [17].

To impart a wider array of properties, itaconic acid derivatives such as poly(dialkyl itaconate)s have provided flexibility in blends or in statistical or block copolymers. For example, di-n-butyl

itaconate (DBI) can impart lower glass transition temperatures in copolymers and consequently similar related dialkyl itaconates have been polymerized via conventional free radical polymerization (FRP) [2,11,18–31] and more recently via reversible de-activation radical polymerization (RDRP), also known as controlled radical polymerization (CRP), specifically reversible addition fragmentation chain transfer polymerization (RAFT) [32,33] and atom transfer radical polymerization (ATRP) [34,35]. In one case, NMP has been reported using TEMPO-based initiators but no molecular weight distributions were provided, ascribed to the styrene/DBI copolymers adsorbing onto the gel permeation chromatography (GPC) columns [36]. Itaconate esters with stiffer substituents like itaconic anhydride have been similarly polymerized by conventional radical polymerization [37–39] and controlled radical polymerizations like RAFT [40] and would be expected to behave similarly to copolymerizations of styrene with maleic anhydride to provide alternating monomer sequences in the chain.

In this report, we present the nitroxide-mediated polymerization (NMP) of DBI/S using the BlocBuilder family of unimolecular initiators to obtain statistical copolymers with enhanced elastomeric properties. These initiators improved upon TEMPO-based initiators in permitting the homopolymerization of acrylates, acrylamides and methacrylates (with a small concentration of controlling co-monomer ~1 mol%–10 mol%), which was not possible with first-generation nitroxides [41]. NMP has often been overlooked compared to RAFT and ATRP as an RDRP process, as witnessed by the case with the itaconate esters. Unlike the RAFT and ATRP systems, very little post-polymerization work-up is required without removal of transition metal ligands or odorous chain transfer agents [41], although these issues have been enormously reduced recently [42–44]. The advantages associated with NMP thus make it worthwhile to evaluate its ability to polymerize itaconate-based monomers, which should be challenging due to the secondary vinylic bond in its structure. Thus, our goal here is to apply NMP to obtain (co)polymers with active chain ends and controllable molecular weight (Scheme 1). We thus studied the polymerizations as a function of temperature, initial compositions and effect of solvent.



Scheme 1. Reaction scheme to copolymerize DBI with S via NMP using NHS-BlocBuilder as initiator.

2. Materials and Methods

2.1. Materials

N-(2-Methylpropyl)-*N*-(1-diethylphosphono-2,2-dimethylpropyl)-*O*-(2-carboxylprop-2-yl) hydroxylamine (99%, BlocBuilder-MATM) was received from Arkema. *N,N'*-Dicyclohexylcarbodiimide (DCC, 99%) was received from Sigma-Aldrich and used in conjunction with BlocBuilder-MATM to synthesize the succinimidyl ester terminated alkoxyamine NHS-BlocBuilder following a procedure previously reported [45]. Tetrahydrofuran (THF, 99.9% HPLC grade), dioxane (99%), methanol (99%) and 1,4-dioxane (99%), were purchased from Fisher Scientific. Styrene (99%, S) was purified to remove the inhibitor by passing through a column of basic alumina mixed with 5 weight% calcium hydride and then stored in a sealed flask under a head of nitrogen in a refrigerator until needed. Di-*n*-butyl itaconate (96%, DBI), dimethyl itaconate (96%, DMI), isobutyramide (99%), calcium hydride (90–95%

reagent) and basic alumina (Brockmann, Type 1, 150 mesh) were purchased from Sigma-Aldrich and used as received. Chloroform-D (99.8%) was obtained from Cambridge Isotope Laboratories.

2.2. DBI/S Copolymerization

The copolymerizations were performed in a 15 mL three-neck round bottom glass flask equipped with a vertical flux condenser, a thermal well and a magnetic Teflon stir bar. The flask was placed on a heating mantle and the equipment was placed on a magnetic stirrer. The condenser was connected to a chilling unit that used a glycol/water mixture (10/90 v/v %) to prevent loss of the monomers and solvent due to evaporation. To the reactor is added the initiator (NHS-BlocBuilder, 0.10 g), 50 wt% solvent (1,4-dioxane), and varying compositions of DBI and S. Once stirring started and the chiller is set to 4 °C, an ultra-pure nitrogen flow was introduced to purge the system for 30 min. An example is used for DBI/S-110-20. In this case, 0.10 g (2.09×10^{-4} mol) of NHS-BlocBuilder was added to 1.59 g DBI (0.066 mol) and 2.73 g (0.0262 mol) of previously purified S along with 5.11 mL of dioxane solvent. A thermocouple was inserted into the temperature well and connected to a controller. The reactor was then heated to the chosen reaction temperature while maintaining the nitrogen purge and stirring with a magnetic stir bar. Table 1 shows the different formulations that were studied. Samples were taken periodically, and once the last sample was taken, 50 mL of methanol was added to the remaining solution to precipitate the polymer. The precipitated polymer was dried overnight in a vacuum oven at 45 °C to remove any remaining solvents or unreacted volatile monomers (styrene). The composition of the copolymer was determined by ^1H NMR using the methyl end groups of DBI and the aromatic styrene protons (ppm, CDCl_3): (t, 0.8–1.05, $\text{CH}_3\text{-CH}_2\text{-CH}_2\text{-}$), (m, 1.2–1.6, backbone and $\text{CH}_3\text{-CH}_2\text{-CH}_2\text{-}$, $\text{CH}_3\text{-CH}_2\text{-CH}_2\text{-}$), (s, 2.7, $\equiv\text{C-CH}_2\text{-COO-}$), (m, 4.2, $\text{COO-CH}_2\text{-CH}_2\text{-CH}_2\text{-CH}_3$), (ar, 6.4–7.7, $\text{-C}_6\text{H}_5$). The molecular weight according to GPC for the specific example was $M_n = 12.3 \text{ kg}\cdot\text{mol}^{-1}$, $\bar{D} = 1.37$, relative to PS standards in THF at 40 °C.

Table 1. Formulations for dibutyl itaconate/styrene (DBI/S) statistical copolymerizations initiated by NHS-BlocBuilder (NHS-BB) at 70–110 °C in 50 wt% 1,4-dioxane solutions.

Sample ID ^a	$f_{\text{DBI},0}$ ^a	T (°C)	[DBI] (M)	[S] (M)	[NHS-BB] (M)	[Dioxane] (M)
DBI/S-110-10	0.10	110	0.41	3.62	0.026	5.54
DBI/S-110-20	0.20	110	0.73	2.91	0.023	5.58
DBI/S-110-30	0.29	110	0.99	2.33	0.021	5.61
DBI/S-110-40	0.40	110	1.22	1.83	0.019	5.64
DBI/S-110-50	0.51	110	1.41	1.41	0.018	5.66
DBI/S-110-60	0.60	110	1.58	1.05	0.017	5.68
DBI/S-110-70	0.71	110	1.72	0.73	0.016	5.69
DBI/S-110-80	0.80	110	1.84	0.46	0.015	5.71
DBI/S-100-50	0.50	100	1.41	1.41	0.018	5.66
DBI/S-80-50	0.50	80	1.41	1.41	0.018	5.66
DBI/S-70-50	0.50	70	1.41	1.41	0.018	5.66
DBI/S-70-60	0.60	70	1.58	1.05	0.017	5.68
DBI/S-70-70	0.70	70	1.72	0.73	0.016	5.69
DBI/S-70-80	0.80	70	1.84	0.46	0.015	5.71
DBI/S-70-90	0.90	70	1.96	0.22	0.014	5.72

^a Sample ID is defined as: DBI/S-XXX-YY = dibutyl itaconate (DBI)/styrene (S) statistical copolymerization at XXX = temperature (°C) and YY = % molar composition of DBI in initial mixture with molar fraction given as $f_{\text{DBI},0}$.

2.3. Chain Extension Experiments

To determine chain end fidelity, chain extension experiments were performed using two macroinitiators, one rich in DBI (DBI/S-110-80; $M_n = 2.60 \text{ kg}\cdot\text{mol}^{-1}$, $\bar{D} = 1.36$) and the other rich in S (DBI/S-110-20, $M_n = 12.3 \text{ kg}\cdot\text{mol}^{-1}$, $\bar{D} = 1.37$). For DBI/S-110-20 as the macroinitiator, typically 1.00 g of macroinitiator was placed inside the reactor with 6.00 g of 1,4 dioxane solvent and 5.00 g of styrene monomer previously purified and mixing started with a magnetic stir bar. The identical

reactors conditions were applied as for the copolymerizations described in Section 2.2. After purging with nitrogen at room temperature for 30 min, the temperature was increased to 110 °C to commence the chain extension. The nitrogen purge remained during the rest of the reaction. Samples were periodically taken to assess the molecular weight distribution. At the conclusion of the polymerization after cooling to < 40 °C, the contents were precipitated into 50 mL of methanol. The precipitated polymer was dried overnight in a vacuum oven at 45 °C to remove any remaining solvents or unreacted volatile monomers (styrene). For DBI/S-110-20 product (DBI-S-110-20-*b*-S) the $M_n = 22\,100\text{ kg mol}^{-1}$, $\bar{D} = 1.61$. A similar procedure was followed using DBI/S-110-80 as the macroinitiator.

2.4. Characterization

Gel permeation chromatography (GPC) was used to obtain molecular weight distributions (MWDs) of the different copolymer samples using HPLC grade THF as the mobile phase. The GPC was calibrated relative to linear PS standards with THF as the eluent at 40 °C. A Waters Breeze GPC system was used at a mobile phase flow rate of $0.3\text{ mL}\cdot\text{min}^{-1}$ equipped with three Styragel HR columns (HR1 with a molecular weight measurement range of 10^2 to $5 \times 10^3\text{ g mol}^{-1}$, HR2 with a molecular weight measurement range of 5×10^2 to $2 \times 10^4\text{ g mol}^{-1}$ and HR4 with a molecular weight measurement range of 5×10^3 to $6 \times 10^5\text{ g mol}^{-1}$) and a guard column. The GPC was equipped with an RI 2410 differential refractive index (RI) detector. For these experiments, the RI detector was used. DBI/S conversion and copolymer composition were determined by ^1H NMR in CDCl_3 . A 300 MHz Varian Gemini 2000 spectrometer was used for the ^1H NMR measurements. Samples were placed in 5 mm up NMR tubes using CDCl_3 as a solvent. After injecting and shimming, the samples were scanned 32 times. Individual conversions were calculated using the integrated areas at $\delta = 6.4\text{--}7.7\text{ ppm}$ for the aromatic protons of styrene and $\delta = 0.8\text{--}1.05\text{ ppm}$ for DBI and taking the reference peaks at 5.3 and 6.1 ppm for the vinyl protons of styrene and DBI, respectively. Once the individual conversion of each monomer was determined, the overall molar conversion was calculated by the following equation: $X_{\text{overall}} = X_S f_{S,0} + X_{\text{DBI}} f_{\text{DBI},0}$, where $f_{S,0}$ and $f_{\text{DBI},0}$ are the initial molar fractions of the monomers and X_S and X_{DBI} are the individual monomer conversions determined from ^1H NMR measurements. Differential scanning calorimetry (DSC) was used to determine the glass transition temperature (T_g) of the various copolymers. A cycle of heat/cool/heat with a heating rate of $10\text{ }^\circ\text{C min}^{-1}$ was performed on the samples and T_g was determined by observing the change in slope in the heat flow (W g^{-1}) versus temperature plot and finding the inflection point using TA Universal Analysis software.

3. Results and Discussion

We first attempted to determine the best conditions for the controlled polymerization of dialkyl itaconates, which is defined here as linear progression of degree of polymerization with monomer conversion, dispersity $\bar{D} (M_w/M_n) < 1.5$ and ability to reinitiate a second batch of monomer. Initially, the homopolymerization of DBI via NMP at different temperatures was examined. Interestingly, although DBI was homopolymerized via conventional radical processes and RDRP processes such as RAFT [32,33] and the related dimethyl itaconate (DMI) by ATRP [34], DBI did not homopolymerize via NMP with no conversion after several hours at elevated temperatures of $\sim 110\text{ }^\circ\text{C}$. We also examined the homopolymerization of dimethyl itaconate (DMI) under the same conditions and again observed no conversion after several hours. We suspected this was due to a stable adduct formed by reaction of the alkoxyamine (NHS-BlocBuilder) and one unit of DBI (see Figure 1). The nature of the C-O-N bond between the alkoxyamine and the monomer is very stable since it is centered on a quaternary carbon, and therefore has a high activation energy barrier to produce the propagating radicals required for subsequent polymerization. During the initiation stage of NMP, when the alkoxyamine is activated for the first time, the initiating radical is produced and reacts with the one monomer unit prior to being deactivated by the nitroxide moiety, rendering the adduct.

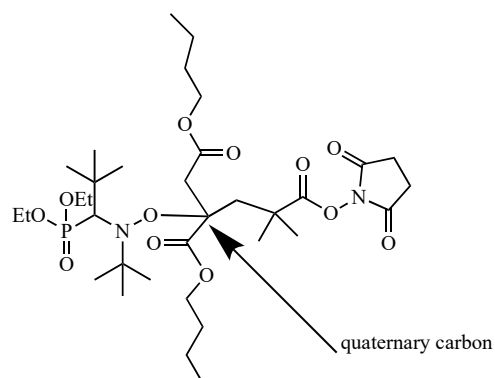


Figure 1. Possible adduct formed during the homopolymerization of dibutyl itaconate (DBI) via NMP with NHS-BlocBuilder.

From other radical polymerizations, the stability of this particular radical is reflected in the much lower k_p of dialkyl itaconates compared to styrenic and (meth) acrylic monomers. For example, PLP-SEC measurements revealed the k_p of DBI $\sim 40 \text{ L mol}^{-1} \text{ s}^{-1}$ at 110°C by extrapolation [46], which is much lower, by comparison to styrene, which has a $k_p \sim 1580 \text{ L mol}^{-1} \text{ s}^{-1}$ at the same temperature [47]. The application of group transfer polymerization (GTP) to dialkyl itaconates revealed only the ability to cap a chain end but no further addition of more monomer units was observed [48,49]. Further, chain transfer to monomer is prevalent in systems with sterically hindered monomers like DBI and were argued to be related to the very low k_p of dialkyl itaconates [50]. In ATRP systems, for DMI with copper halides teamed with various ligands such as methyl 2-bromopropionate (MBrP), *p*-toluene 2-sulfonyl chloride, pentamethyl diethylenetriamine (PMDETA) and 2,2'-bipyridine (bpy) at temperatures of 100°C and 120°C , were controlled up to about 50% conversion, with an abrupt decrease in polymerization rates at that juncture [34]. These variations did not enhance polymerization rate or control of the polymerization. Later, Hirano et al. employed ATRP of DBI at 60°C ; higher temperatures resulted in intramolecular chain transfer [25]. This same group continued to try to increase the rate of reaction by using hydrogen bonding and Lewis acids [26,27]. In RAFT systems, a variety of CTAs were applied, and poly(DBI) could be homopolymerized in a controlled fashion at low temperatures of $\sim 20^\circ\text{C}$, which likely suppressed many transfer reactions, although rate of polymerization was compromised (e.g., 150 h to obtain 50% conversion) and generally fairly low molecular weights resulted [33]. Thus, our experiments generally matched that observed previously, but NMP of dialkyl itaconates did not result in polymer with appreciable molecular weight, compared to ATRP and RAFT processes. We thus turned our attention to binary copolymerization systems with a monomer that is easily polymerizable by NMP: styrene.

We performed copolymerizations of DBI with S ($f_{\text{DBI},0} = 0.1$ to 0.8) at 110°C , as NMP of styrenic-based monomers is well controlled and relatively fast at such temperatures [51]. We attempted to see if the polymerization kinetics we observed would approach those predicted for NMP of model copolymerizations. Semi-logarithmic kinetic plots of the different copolymerizations ($\ln(1/(1 - X))$ versus time) were used to extract the apparent rate constant, $\langle k_p \rangle [P\cdot]$ from the slope, where $\langle k_p \rangle$ is the compositionally averaged propagation rate constant and $[P\cdot]$ is the concentration of the active chains. Such a plot would be expected to be linear.

$$\ln\left(\frac{1}{1 - X}\right) = k_p [P\cdot] t \quad (1)$$

We would expect the propagation rate to vary as a function of the copolymerization feed. The propagation rate constant that we are measuring is actually an average rate constant that is dependent on the individual propagation rate constants and the reactivity ratios as exemplified for a terminal kinetic model (since reactivity ratio data was available for the DBI/S pair) in Equation (2)

where r_1 and r_2 are the reactivity ratios of monomers 1 and 2, f_1 and f_2 are the respective molar fractions of the monomer mixture and k_{11} and k_{22} refer to the individual homopropagation rate constants [52].

$$\langle k_p \rangle = \frac{r_1 f_1^2 + 2f_1 f_2 + r_2 f_2^2}{\frac{r_1 f_1}{k_{11}} + \frac{r_2 f_2}{k_{22}}} \quad (2)$$

The steady-state concentration of radical ended chains, is provided by Fischer's expression [53]:

$$[P\cdot] = \left(\frac{\langle K \rangle [I]_0}{3 \langle k_t \rangle} \right)^{1/3} t^{-1/3} \quad (3)$$

where $\langle K \rangle$ is the average equilibrium constant, $[I]_0$ is the initiator concentration, $\langle k_t \rangle$ is the average termination rate constant and time is given by t . Further, $\langle K \rangle$ assuming a terminal model, was provided by Charleux and co-workers in Equation (4) [54].

$$\langle K \rangle = \frac{\frac{r_1 f_1}{k_{11}} + \frac{r_2 f_2}{k_{22}}}{\frac{r_1 f_1}{k_{11} K_1} + \frac{r_2 f_2}{k_{22} K_2}} \quad (4)$$

Here, the individual reactivity ratios, monomer molar fractions and individual homopropagation rate constants are defined as above while K_1 and K_2 are the individual equilibrium constants. The termination rate constant is provided by the following [55]:

$$\langle k_t \rangle = \left(p_1 k_{t,1}^{1/2} + p_2 k_{t,2}^{1/2} \right)^2, \quad (5)$$

where:

$$p_1 = \frac{\frac{r_1 f_1}{k_{11}}}{\frac{r_1 f_1}{k_{11}} + \frac{r_2 f_2}{k_{22}}} \text{ and } p_2 = 1 - p_1 \quad (6)$$

For the terminal model, all of the parameters are available, with the exception of the K for DBI, to predict the apparent rate constant $\langle k_p \rangle [P\cdot]$, which can be compared to our experimental values. Thus, reactivity ratios are used from DBI/S conventional radical copolymerizations at 60 °C in benzene ($r_{\text{DBI}} = 0.38 \pm 0.02$ and $r_S = 0.40 \pm 0.05$; [19] while the propagation rate constants at 110 °C for DBI and S being $k_{p,\text{DBI}} = 40 \text{ L}\cdot\text{mol}^{-1}\cdot\text{s}^{-1}$ [46] and $k_{p,S} = 1580 \text{ L}\cdot\text{mol}^{-1}\cdot\text{s}^{-1}$ [47], respectively. The K_S is estimated to be $1.1 \times 10^{-9} \text{ s}^{-1}$ at 110 °C [51,56] while individual termination rate constants at 110 °C are estimated to be $k_{t,\text{DBI}} = 1.4 \times 10^6 \text{ L}\cdot\text{mol}^{-1}\cdot\text{s}^{-1}$ [57] and $k_{t,S} = 1.5 \times 10^8 \text{ L}\cdot\text{mol}^{-1}\cdot\text{s}^{-1}$ [58]. As $f_{\text{DBI},0}$ is increased, the experimental $\langle k_p \rangle [P\cdot]$ did not vary much. Iterating on K_{DBI} to try to fit the data only resulted in good agreement between the experimental and predicted relationship at high $f_{\text{DBI},0}$ (Figure 2). There are several possible explanations for the disagreement. First, there could indeed be a strong penultimate effect as was suggested by Yee et al. [59]. For DMI/S copolymerizations, the terminal model for the $\langle k_p \rangle$ did not match the experimental data very well. We suspect that a similar effect was occurring in the DBI/S system. Further, Yee et al. found that the terminal group was nearly always DMI up to very high styrene content (~80 mol%) [59]. They found that this particular pair had a strong penultimate unit effect on the copolymerization propagation rate constant and the measured average propagation rate constant was about three times higher than that predicted by the terminal model. In RAFT and ATRP, the same stability of the dialkyl itaconate was noted and further it was stated that the polymerization of DBI or DMI was not a truly reversible deactivation polymerization process and was indeed a mixture between conventional and controlled polymerization [60].

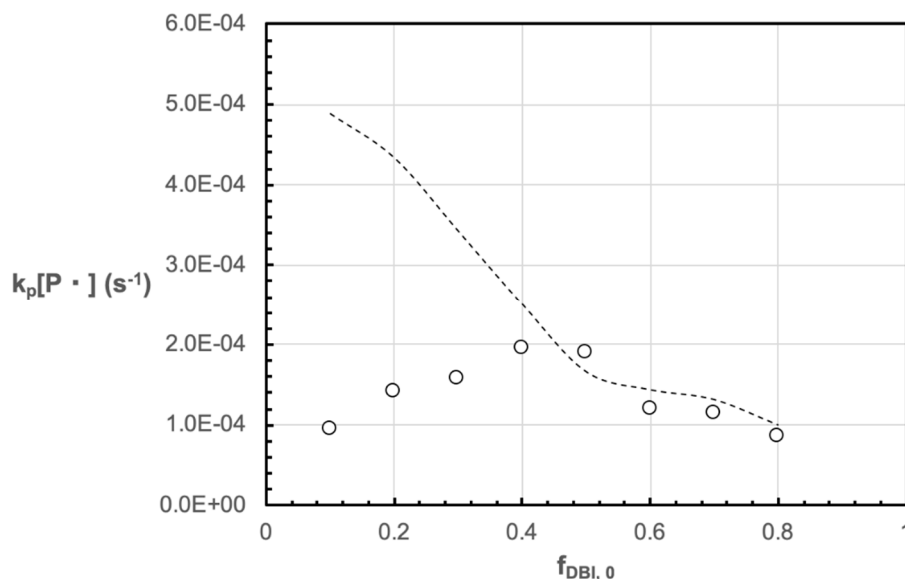


Figure 2. Apparent rate constant $k_p[P\cdot]$ as a function of initial molar composition of dibutyl itaconate, $f_{\text{DBI},0}$, for DBI/S copolymerizations at 110 °C in 50 wt% dioxane solutions. The dashed lines indicate the prediction for $k_p[P\cdot]$ based on the terminal model for the copolymerization.

The M_n versus conversion plots are shown in Figure 3 where Figure 3a plots polymerizations with initial feed compositions of $f_{\text{DBI},0} = 0.1$ – 0.4 while Figure 3b plots polymerizations with initial feed compositions of $f_{\text{DBI},0} = 0.5$ – 0.8 . For low initial loadings of DBI such as for $f_{\text{DBI},0} = 0.10$ and 0.20 , M_n increased linearly with X . However, experiments with $f_{\text{DBI},0} > 0.20$ (Figure 3b), plateauing of the M_n became increasingly evident. (full data set of M_n , M_w , individual conversion of the copolymerizations carried out at 110 °C are shown in Table S1 of the Supporting Information).

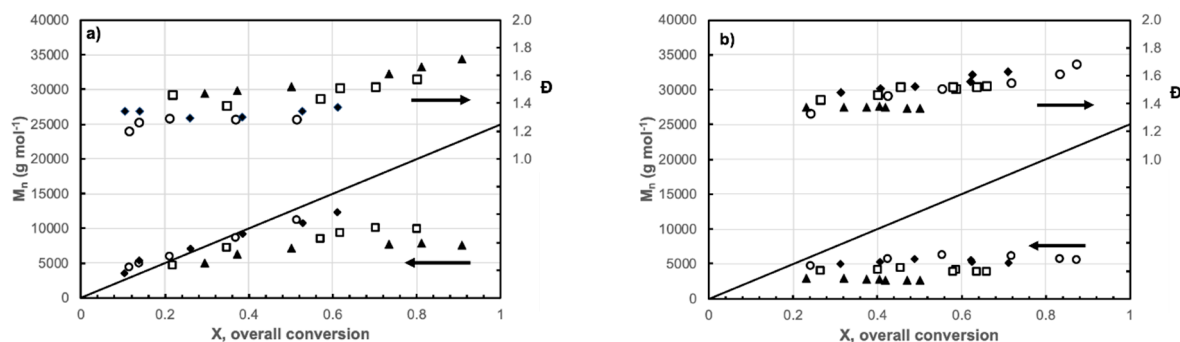


Figure 3. Number average molecular weight M_n and dispersity \bar{D} versus overall conversion (X) for DBI/S copolymerization at (a) initial molar compositions of DBI $f_{\text{DBI},0} = 0.1$ – 0.4 ($f_{\text{DBI},0} = 0.1$ are open circles \circ , $f_{\text{DBI},0} = 0.2$ are solid diamonds \blacklozenge , $f_{\text{DBI},0} = 0.3$ are open squares \square , and $f_{\text{DBI},0} = 0.4$ are solid triangles \blacktriangle) and at (b) initial molar compositions of DBI $f_{\text{DBI},0} = 0.5$ – 0.8 ($f_{\text{DBI},0} = 0.5$ are open circles \circ , $f_{\text{DBI},0} = 0.6$ are solid diamonds \blacklozenge , $f_{\text{DBI},0} = 0.7$ are open squares \square , and $f_{\text{DBI},0} = 0.8$ are solid triangles \blacktriangle).

One of the reasons for this behavior can be attributed to the high affinity of the itaconate monomer to be involved in chain transfer reactions [18,25]. For a DBI conventional free radical polymerization, the chain-transfer reaction occurs when the propagating radical abstracts a hydrogen atom from a monomer unit, yielding an end-saturated polymer chain and a new monomeric radical [18]. Later, Hirano and Takayoshi suggested that at temperatures higher than 60 °C, intramolecular chain-transfer reactions are favored [25]. They argued that this happens due to the formation of a less stable secondary radical from a more stable tertiary radical, which requires a higher activation energy than the propagating reaction [25]. In an NMP process, intramolecular chain-transfer reactions might occur

when the chains are active. Hirano and Takayoshi also suggested that chain-transfer reactions can be suppressed by a reversible deactivation process such as ATRP [25]. However, in the NMP process, the reactivation of the polymer chains depends on the homolysis capability of the C-O-N bond formed between the alkoxyamine and the DBI monomer unit as previously discussed. Together with the irreversible chain termination reactions that occur inevitably, the chain transfer/termination becomes more prominent at higher DBI initial compositions. As illustrated in Figure 3b, when $f_{\text{DBI},0} > 0.5$, the M_n is almost constant at any conversion and as $f_{\text{DBI},0}$ the plateau M_n decreases (as these reactions happen more frequently and earlier). These same trends are shown in the GPC chromatograms in Figure 4. At $f_{\text{DBI},0} < 0.3$, the molecular weight distributions shift steadily to higher molecular weight while propagation is essentially stopped for $f_{\text{DBI},0} > 0.6$ with only a few monomeric units added on as the M_n listed in Table 2 (from GPC relative to PS standards) indicate.

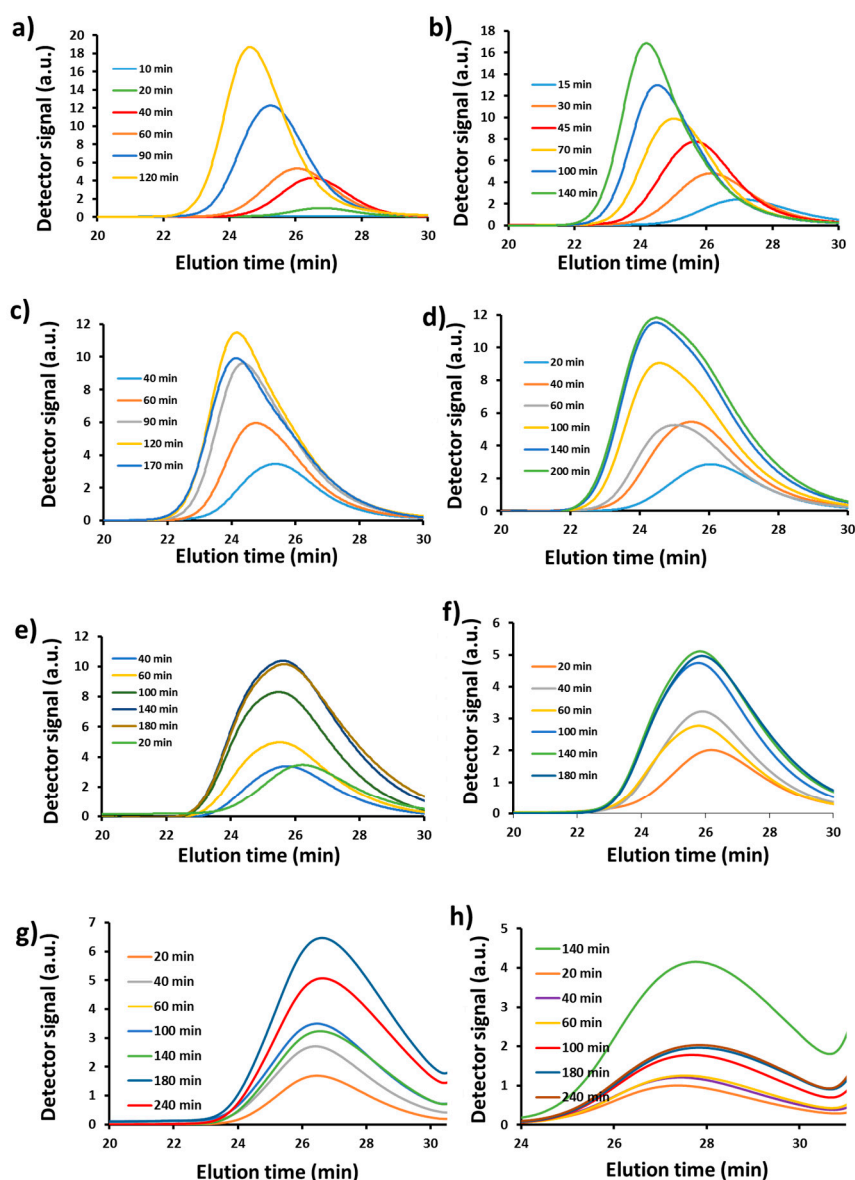


Figure 4. GPC traces (elution time) of DBI-S copolymerizations done at 110 °C.: (a) $f_{\text{DBI},0} = 0.1$, (b) $f_{\text{DBI},0} = 0.2$, (c) $f_{\text{DBI},0} = 0.3$, (d) $f_{\text{DBI},0} = 0.4$, (e) $f_{\text{DBI},0} = 0.5$, (f) $f_{\text{DBI},0} = 0.6$, (g) $f_{\text{DBI},0} = 0.7$, (h) $f_{\text{DBI},0} = 0.8$.

Table 2. Summary of dibutyl itaconate/styrene copolymerizations in 50 wt% dioxane solution at 110 °C.

Sample ID ^a	$f_{\text{DBI},0}$	Time (min)	X ^b	F_{DBI} ^c	M_n (kg mol ⁻¹) ^d	\bar{D} ^d
DBI/S-110-10	0.10	120	0.51	0.13	11.2	1.28
DBI/S-110-20	0.20	140	0.61	0.25	12.3	1.37
DBI/S-110-30	0.29	170	0.80	0.30	9.9	1.57
DBI/S-110-40	0.40	200	0.91	0.40	7.6	1.72
DBI/S-110-50	0.51	180	0.87	0.45	5.5	1.68
DBI/S-110-60	0.60	180	0.71	0.50	5.0	1.62
DBI/S-110-70	0.71	230	0.75	0.60	3.7	1.52
DBI/S-110-80	0.80	240	0.50	0.65	2.6	1.36

^a Sample ID is defined as: DBI/S-XXX-YY = dibutyl itaconate (DBI)/styrene (S) statistical copolymerization at XXX = temperature (°C) and YY = % molar composition of DBI in initial mixture with molar fraction given as $f_{\text{DBI},0}$. ^b X = overall molar conversion. ^c The final copolymer composition with respect to DBI is given as F_{DBI} and determined by ¹H NMR. ^d Number average molecular weight M_n and dispersity \bar{D} determined by GPC relative to poly(styrene) standards in THF at 40 °C.

With the apparent loss of control with copolymerizations richer in DBI, we carried out a study of copolymerizations of DBI/S (50/50 mol%) at lower temperatures of 100, 80 and 70 °C and compared the results observed at the same composition at 110 °C in order to determine if lower temperature might reduce the possible intramolecular chain transfer reactions. Figure 5 shows the M_n versus overall conversion plots for the DBI/S copolymerizations ($f_{\text{DBI},0} = 0.5$) done at 110, 100, 80 and 70 °C. Table 3 also summarizes the various properties for these equimolar copolymerizations. Indeed, temperature is a factor that affects the overall conversion and it was therefore necessary to run reactions for longer at lower temperatures. For example, conversion was close to 90% in only 180 min at 110 °C but at 70 °C, overall conversion was only 47% after three days. There seemed to be only slight improvement, but the molecular weight did not plateau as early as with polymerizations done at higher temperatures. This observation is supported by the GPC traces in Figure 6, which shows the polymerization at 70 °C continually growing whereas at 110 °C, the polymerization was effectively stopped.

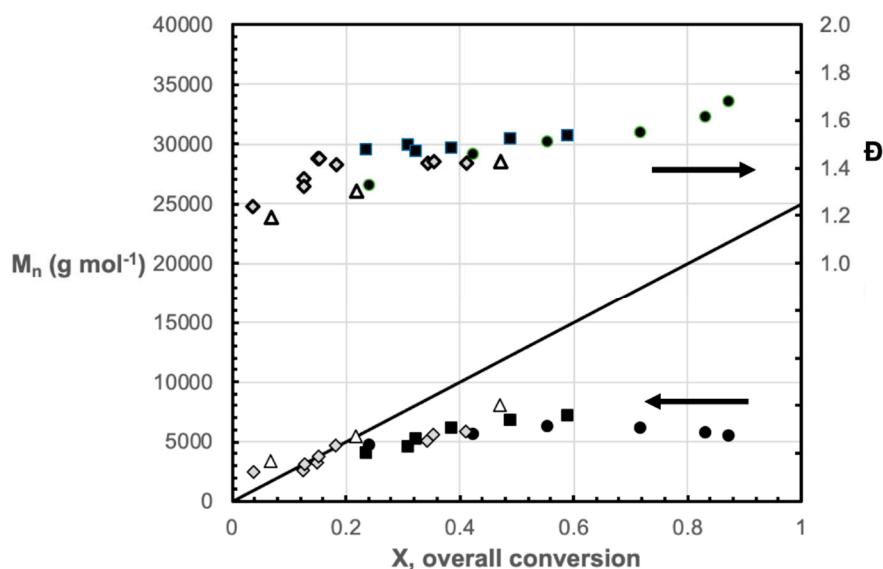


Figure 5. Number average molecular weight M_n and dispersity \bar{D} versus overall conversion (X) for DBI/S copolymerizations at composition $f_{\text{DBI},0} = 0.5$ at various temperatures: at (a) 110 °C (filled circles ●), (b) 100 °C (filled squares ■), (c) 80 °C (open diamonds ◊) and (d) 70 °C (open triangles △).

Table 3. Summary of equimolar dibutyl itaconate/styrene copolymerizations in 50 wt% dioxane solution at various temperatures.

Sample ID ^a	$f_{\text{DBI},0}$	Time (min)	X ^b	M_n (kg mol ⁻¹) ^c	\bar{D} ^c
DBI/S-110-50	0.51	180	0.87	5.5	1.68
DBI/S-100-50	0.50	180	0.59	7.1	1.53
DBI/S-80-50	0.50	340	0.41	5.8	1.42
DBI/S-70-50	0.50	4320	0.47	8.0	1.42

^a Sample ID is defined as: DBI/S-XXX-YY = dibutyl itaconate (DBI)/styrene (S) statistical copolymerization at XXX = temperature (°C) and YY = % molar composition of DBI in initial mixture with molar fraction given as $f_{\text{DBI},0}$.

^b X = overall molar conversion. ^c Number average molecular weight M_n and dispersity \bar{D} determined by GPC relative to poly(styrene) standards in THF at 40 °C.

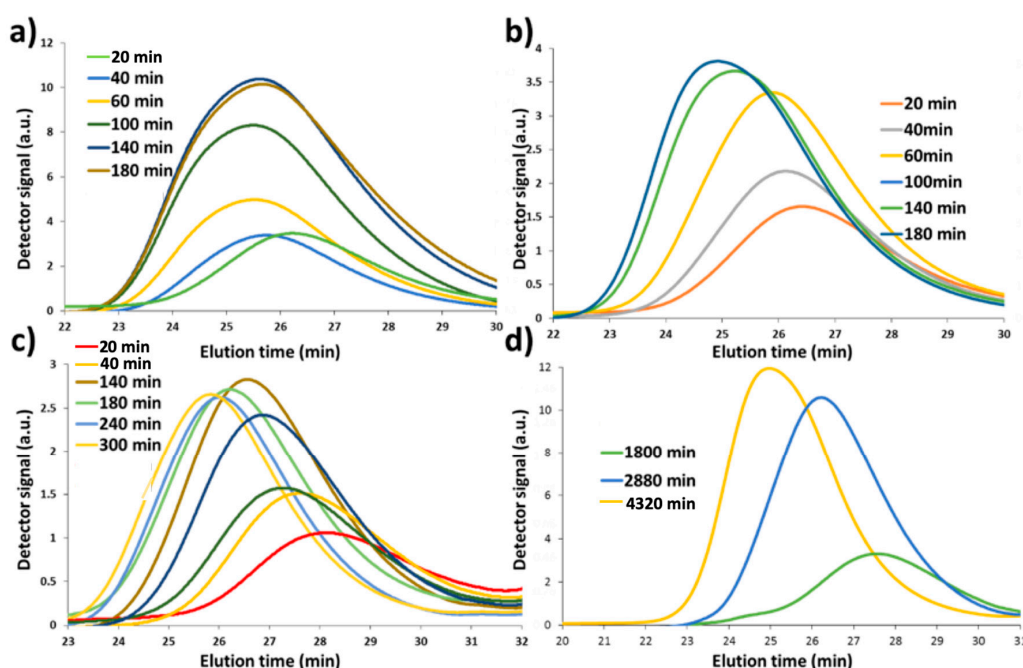
**Figure 6.** GPC traces of DBI-S copolymerizations ($f_{\text{DBI},0} = 0.50$ in all cases) done at (a) 110 °C, (b) 100 °C, (c) 80 °C and (d) 70 °C.

Table S2 in the Supporting Information shows the individual conversion of DBI and S, M_n , M_w and \bar{D} for DBI-S copolymerizations (50–50 mol%) done at 110, 100, 80 and 70 °C. In every case, the conversion of S was higher than DBI, meaning that the final composition of the copolymers is richer in S than DBI. The GPC traces of the copolymerizations for DBI-S (50–50 mol%) done at 110, 100, 80 and 70 °C are shown in Figure 6. Although at 110 °C almost full conversion was achieved at relatively shorter times, the GPC traces at this temperature (Figure 6a) showed little growth towards higher chain lengths [41] and the same molecular weight distribution from the early stages of the reaction just became broader during the course of the reaction. Although the conversion did increase linearly with time, this might be due to the chain transfer and termination of chains with the formation of low molecular weight chains. The GPC traces of the reactions at 100 °C and 80 °C moved towards higher molecular weight only at the early stages of the reactions (low conversion) and low molecular weight tailing was still observed, followed by no further increase in molecular weight after about 30% conversion. At 70 °C, although the reaction took longer to reach 40% conversion ~ 2 days, it showed shifting towards higher molecular weight and very little tailing. As noted earlier for the radical polymerization of DBI, intramolecular chain transfer side reactions take place at high temperatures [25] which was corroborated by our DBI/S copolymerizations at $f_{\text{DBI},0} = 0.50$. We thus focused on copolymerizations at the lower temperature of 70 °C for three days to see if the mixtures with higher DBI loadings led to higher molecular weight polymers.

As observed from Figure 5, with decreasing temperature, the M_n versus conversion slightly shifts up toward the theoretical line which shows intramolecular chain transfer reactions can be mitigated to some degree by decreasing temperature. The control of the polymerizations seems to be better at 70 °C. At this temperature, as the compositions become richer in DBI, the M_n versus conversion plots do rise but still become noticeably flatter with conversion (Table 4 summarizes the copolymerizations while Figure 7 shows M_n versus conversion and individual conversions are listed in Table S3 of Supporting Information). The GPC chromatograms for experiments with $f_{DBI,0} = 0.60, 0.70$ and 0.80 at 70 °C show clear shifts towards higher molecular weights (Figure 8). Only in the case of $f_{DBI,0} = 0.90$ do the GPC traces show no growth. Also, it is worth mentioning that the obtained molecular weight is still much lower than the expected value. The main reason could be that the maximum temperature of the reaction which is suggested by Hirano and Tayoshi is 60 °C, which was not tested in our experiment due to the minimum temperature required for NHS-BlocBuilder dissociation ($T \geq 65$ °C) [61]. Thus, DBI/S copolymerizations can be pushed to higher initial DBI compositions > 50 mol%, provided the polymerization temperature does not decrease < 65 °C. Another issue regarding the differences between the actual and theoretical molecular weights is the difference in hydrodynamic volume from GPC measurements. All of the GPC measurements here were measured relative to PS standard in THF. For poly(DBI), no Mark-Houwink-Sakurada (MHS) parameters were available for THF but MHS parameters for poly(DBI) in THF were reasonably approximated by those for poly(DBI) in toluene at similar temperatures ($K = 5.7 \times 10^{-3} \text{ mL g}^{-1}$, $a = 0.70$ at 25 °C) [62]. These MHS parameters are similar to PS in THF at 25 °C ($K = 14.1 \times 10^{-3} \text{ mL g}^{-1}$, $a = 0.70$ at 25 °C) [63]. The differences in hydrodynamic volume would not be very significant between PS and poly (DBI) and would not be solely responsible for the flattening of the M_n versus conversion plots for the copolymerizations performed.

Table 4. Summary of dibutyl itaconate/styrene copolymerizations in 50 wt% dioxane solution at 70 °C at different initial compositions.

Sample ID ^a	$f_{DBI,0}$	Time (min)	χ ^b	M_n (kg mol ⁻¹) _c	\bar{D} ^c
DBI/S-70-60	0.60	4320	0.56	6.9	1.63
DBI/S-70-70	0.70	4320	0.58	7.2	1.41
DBI/S-70-80	0.80	4320	0.66	5.9	1.33
DBI/S-70-90	0.90	4320	0.38	3.2	1.38

^a Sample ID is defined as: DBI/S-XXX-YY = dibutyl itaconate (DBI)/styrene (S) statistical copolymerization at XXX = temperature (°C) and YY = % molar composition of DBI in initial mixture with molar fraction given as $f_{DBI,0}$. ^b χ = overall molar conversion. ^c Number average molecular weight M_n and dispersity \bar{D} determined by GPC relative to poly(styrene) standards in THF at 40 °C.

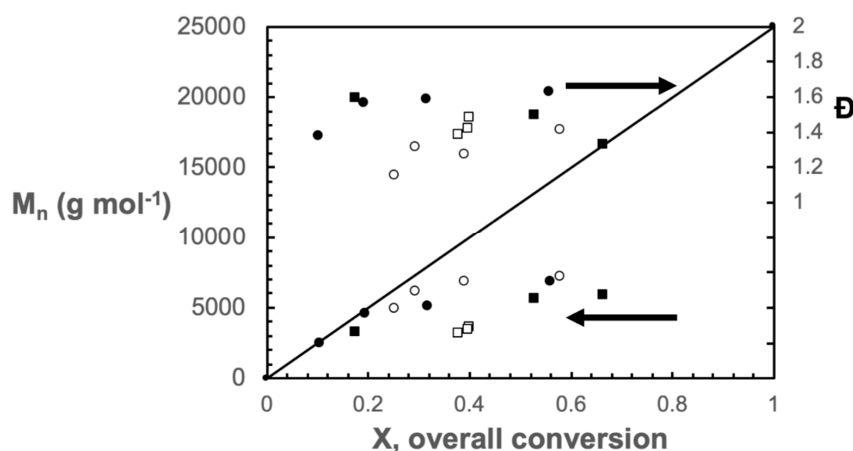


Figure 7. Number average molecular weight M_n versus overall conversion (X) for DBI/S copolymerization with initial DBI feed compositions $f_{DBI,0} = 0.60$ – 0.90 done at 70 °C: $f_{DBI,0} = 0.6$ (filled circles, ●); $f_{DBI,0} = 0.7$ (open circles, ○); $f_{DBI,0} = 0.8$ (filled squares, ■), $f_{DBI,0} = 0.9$ (open squares, □).

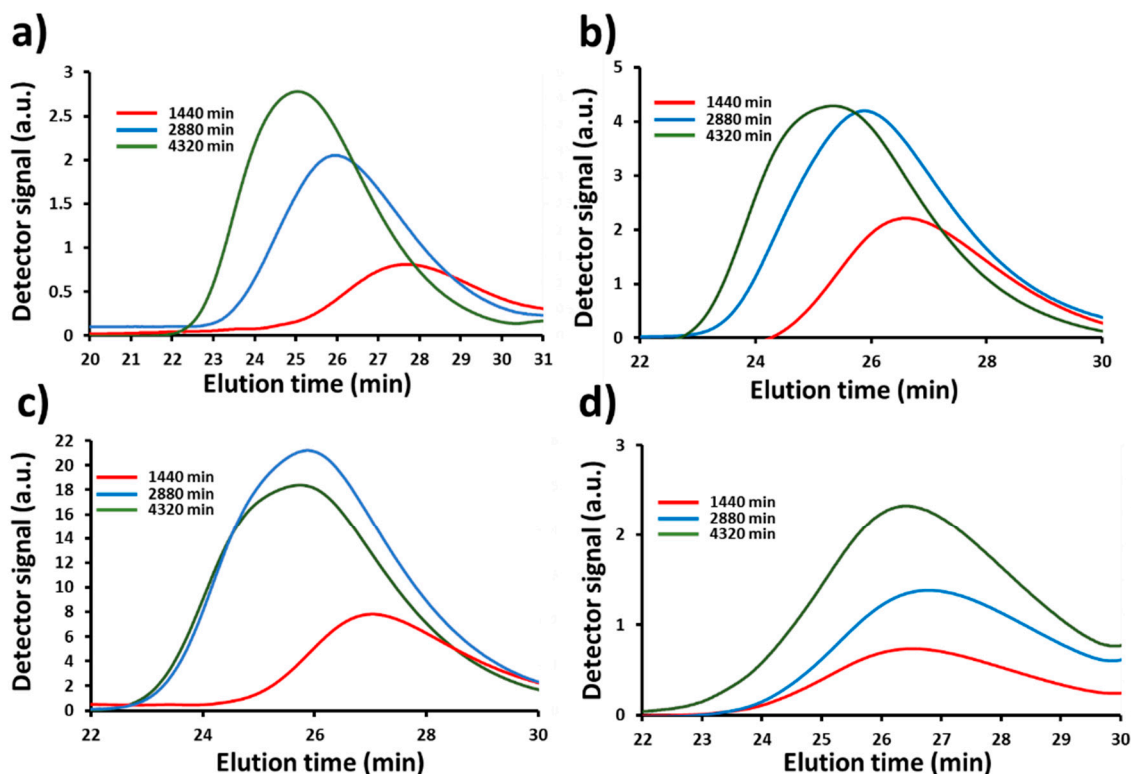


Figure 8. GPC traces (elution time) of DBI-S copolymerizations at 70 °C at (a) $f_{\text{DBI},0} = 0.60$, (b) $f_{\text{DBI},0} = 0.70$, (c) $f_{\text{DBI},0} = 0.80$ and (d) $f_{\text{DBI},0} = 0.90$.

It should be stated that we attempted further DBI copolymerizations with methyl methacrylate (MMA) using NHS-BlocBuilder with little avail at temperatures between 90 and 110 °C. It is likely that the nitroxide adduct with DBI is too stable even when using a monomer like MMA that has a higher k_p compared to S at similar temperatures.

Finally, chain extension experiments with S using a P(DBI/S) macroinitiator were done: S-rich ($f_{\text{DBI},0} = 0.2$) or DBI-rich ($f_{\text{DBI},0} = 0.8$) macroinitiators were used from the copolymerizations done at 110 °C (Table 5 summarizes the chain extensions). In a typical NMP system, it is well-established that <10% of the polymer chains are irreversibly terminated, which means that >90% of the chains are end-functionalized with nitroxide moieties capable of reactivation to allow extension of the polymer chains [41]. The main objective of these experiments was to confirm our previous discussions, specifically if the DBI-rich macroinitiator could be re-activated and add the second batch of monomer. Figure 9a shows the GPC traces of the chain extension experiment using a macroinitiator with $f_{\text{DBI},0} = 0.2$.

Table 5. Summary of chain extension reactions of dibutyl itaconate/styrene (DBI/S) macroinitiators with styrene at 110 °C in 50 wt% dioxane solution.

Experiment	Macroinitiator		Product	
	M_n (kg mol ⁻¹)	\bar{D}	M_n (kg mol ⁻¹)	\bar{D}
DBI/S-110-20-b-S	12.3	1.37	22.1	2.99
DBI/S-110-80-b-S	2.6	1.36	19.2	1.61

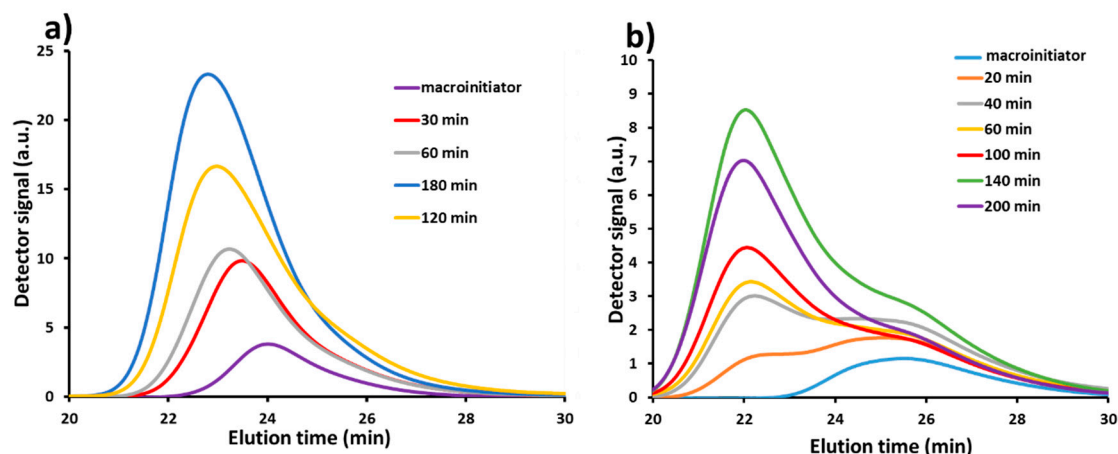


Figure 9. GPC traces (elution time) of DBI-S chain extension experiments with S at 110 °C using a macroinitiator P(DBI-S) a) $f_{\text{DBI},0} = 0.20$ and b) $f_{\text{DBI},0} = 0.80$.

As expected, shifts towards higher molecular weights were observed with time, but also some tailing, meaning that most of the polymer chains end-capped with SG1 did extend. When the macroinitiator from a feed of $f_{\text{DBI},0} = 0.8$ was used, the GPC traces (Figure 9b) exhibited some shifting to higher molecular weight with time, but each trace had a very pronounced shoulder, confirming that most of the polymer chains are either terminated or are not capable to be reactivated again.

One of the potential applications of poly (dialkyl itaconates) is as a component in thermoplastic elastomers. They can be copolymerized in much the same way as dienes are with monomers like styrene to afford tough but flexible materials. The reactivity ratios for the DBI/S system by conventional radical polymerization were reported previously in benzene at 60 °C ($r_{\text{DBI}} = 0.38 \pm 0.02$ and $r_{\text{S}} = 0.40 \pm 0.05$ [19]. In the same study, reactivity ratios were similar for other di-n-alkyl itaconates (DXI where X = methyl, n-ethyl, n-propyl, n-amyl and n-octyl) ($r_{\text{DXI}} = 0.25\text{--}0.60$, $r_{\text{S}} = 0.25\text{--}0.40$). More recently, others have extended the analysis to higher di-n-alkyl itaconates ($n = 12, 14, 16, 18$ and 22) in bulk conventional free radical polymerization at 60 °C using AIBN initiator [28]. For $n = 12, 14, 16$, reactivity ratios for di-n-alkyl itaconate ranged from $0.22\text{--}0.28$ and $r_{\text{S}} = 0.19\text{--}0.39$ while for $n = 18$ and 22 , $r_{\text{DXI}} = 0.42\text{--}0.50$ and $r_{\text{S}} = 0.37\text{--}0.47$. Similar ranges in reactivity ratios were observed for DMI/S copolymerizations although there was considerable spread in the data (Davis and co-workers found that DMI was contaminated with poly (DMI) [59]. Our data, after fitting with Fineman-Ross and Kelen-Tudos methods, revealed $r_{\text{DBI}} = 0.29$ and $r_{\text{S}} = 0.59$ and $r_{\text{DBI}} = 0.32$ and $r_{\text{S}} = 0.77$, respectively. A non-linear least square fitting to the Mayo-Lewis equation provided $r_{\text{DBI}} = 0.31$ and $r_{\text{S}} = 0.61$.

Given that conditions for obtaining higher loadings of DBI are accessible, it would be possible now to tune the desired glass transition temperature (T_{g}) of the copolymers, which was measured using differential scanning calorimetry (DSC). The variation in T_{g} with composition is bracketed by the T_{g} s of the homopolymers ($T_{\text{g,PS}}$ are 100 °C [64] while the $T_{\text{g,PDBI}}$ has been reported to vary between 5–17 °C [22,30,65,66]). Figure 10 shows the T_{g} of the various statistical copolymers as function of final copolymer composition as well as the Fox equation prediction, which is given in Equation (7) where w_{DBI} and w_{S} are the weight fractions of DBI and S and $T_{\text{g,PDBI}}$ and $T_{\text{g,PS}}$ are the experimental T_{g} s of PDBI and PS homopolymers.

$$1/T_{\text{g,th}} = w_{\text{DBI}}/T_{\text{g,PDBI}} + w_{\text{S}}/T_{\text{g,PS}} \quad (7)$$

Although the fit to the Flory-Fox equation is not particularly good, it is still clear that even having a low fraction of DBI in the copolymer was able to dramatically reduce the T_{g} . For example, a copolymer with composition $F_{\text{DBI}} = 18$ mol% had a T_{g} of 45 °C, much lower than the T_{g} of the PS homopolymer (~100 °C). This is due to the flexibility that DBI provided to the polymer chains, giving additional free volume and thus a dramatic decrease in the T_{g} . The copolymers were noticeably more flexible with increasing DBI composition.

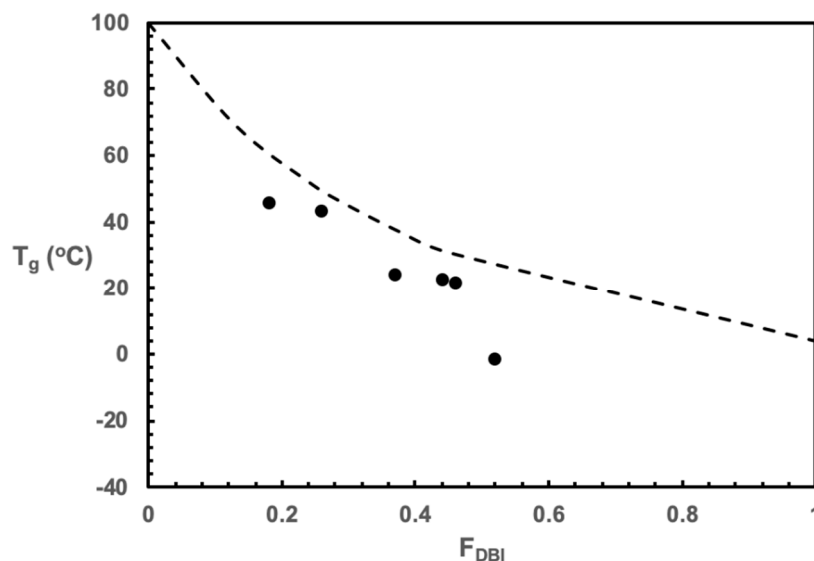


Figure 10. F_{DBI} effects on T_g in P(DBI-S) statistical copolymers. The Fox equation prediction of the P(DBI-S) T_g are represented by the dotted line while the experimental data is presented by the solid circles.

4. Conclusions

In this study, nitroxide-mediated copolymerization of DBI with S was studied using the succinimide functionalized NHS-BlocBuilder at different temperatures. It was not possible to obtain homopolymers of PDBI by NMP, likely due to the formation of a stable adduct, effectively blocking further propagation. When DBI was copolymerized with styrene-rich initial compositions ($f_{DBI,0} < 0.2$) at 110 °C, M_n versus conversion plots were relatively linear up to fairly high conversion ~ 0.6 with relatively narrow molecular weight distributions ($\bar{D} = 1.3\text{--}1.4$). At $f_{DBI,0} > 0.2$, M_n versus conversion plots flattened with increasing conversion and M_n was much lower than theoretical predictions, indicating the high tendency of itaconate monomers to generate intramolecular chain transfer side reactions and the increased probability for formation of stable adducts. A change in reaction temperature to 70 °C indicated a slight improvement in terms of control (narrowed molecular weight distributions and M_n versus conversion remained linear up to higher conversions). This however was accompanied by excessively long polymerization times of around three days. DSC was used to measure the T_g of the copolymers. As expected, T_g decreased as composition of DBI in the copolymer increased, leading the material to become less rigid than the PS homopolymer.

Supplementary Materials: The following are available online at <http://www.mdpi.com/2227-9717/7/5/254/s1>, Tables S1, S2 and S3 indicating individual monomer conversions and molecular weight data are listed.

Author Contributions: Conceptualization, M.M., O.G.V. and A.M.; methodology, O.G.V., M.M.; formal analysis, S.K.; O.G.V., A.M., M.M.; investigation, S.K., O.G.V., A.M.; data curation, S.K.; writing—Original draft preparation, S.K.; writing—Review and editing, M.M., A.M.; supervision, M.M.; project administration, M.M.; funding acquisition, M.M.

Funding: This research was funded by an NSERC Discovery Grant, grant number 288125 (M.M.).

Acknowledgments: We would like to thank Arkema (Mickael Havel and Noah Macy) particularly for their help in providing the BlocBuilder and SG1 initiators described in this work.

Conflicts of Interest: The authors declare no conflict of interest.

References

- Robert, T.; Friebe, S. Itaconic acid—A versatile building block for renewable polyesters with enhanced functionality. *Green Chem.* **2016**, *18*, 2922–2934. [CrossRef]
- Tate, B.E. Polymerization of itaconic acid and derivatives. *Adv. Poly. Sci.* **1967**, *5*, 214–232.

3. Velada, J.; Hernáez, E.; Cesteros, L.C.; Katime, I. Study of the thermal degradation of several poly (monoalkylaryl itaconates). *Polym. Degrad. Stab.* **1996**, *52*, 273–282. [CrossRef]
4. Calam, C.T.; Oxford, A.E.; Raistrick, H. Studies in the biochemistry of micro-organisms: Itaconic acid, a metabolic product of a strain of *Aspergillus terreus* Thom. *Biochem. J.* **1939**, *33*, 1488. [CrossRef] [PubMed]
5. Willke, T.; Vorlop, K.-D. Biotechnological production of itaconic acid. *Appl. Microbiol. Biotechnol.* **2001**, *56*, 289–295. [CrossRef]
6. Willke, T.; Vorlop, K.-D. Industrial bioconversion of renewable resources as an alternative to conventional chemistry. *Appl. Microbiol. Biotechnol.* **2004**, *66*, 131–142. [CrossRef]
7. Dai, J.; Liu, X.; Ma, S.; Wang, J.; Shen, X.; You, S.; Zhu, J. Soybean oil-based UV-curable coatings strengthened by crosslink agent derived from itaconic acid together with 2-hydroxyethyl methacrylate phosphate. *Prog. Org. Coat.* **2016**, *97*, 210–215. [CrossRef]
8. Katime, I.; Rodríguez, E. Absorption of metal ions and swelling properties of poly (acrylic acid-co-itaconic acid) hydrogels. *J. Macromol. Sci. Part A Pure Appl. Chem.* **2001**, *38*, 543–558. [CrossRef]
9. Werpy, T.; Petersen, G.; Aden, A.; Bozell, J.; Holladay, J.; White, J.; Manheim, A. *Top Value Added Chemicals from Biomass Vol. I—Results of Screening for Potential Candidates from Sugars and Synthesis Gas*; Report DOE/GO-102004-1992; U.S. Department of Energy, Office of Scientific and Technical Information: Washington, DC, USA, 2004. Available online: <https://www.nrel.gov/docs/fy04osti/35523.pdf> (accessed on 30 April 2019).
10. Klement, T.; Büchs, J. Itaconic Acid—A Biotechnological Process in Change. *Bioresour. Technol.* **2013**, *135*, 422–431. [CrossRef]
11. Marvel, C.S.; Shepherd, T.H. Polymerization Reactions of Itaconic Acid and Some of Its Derivatives. *J. Org. Chem.* **1959**, *24*, 599–605. [CrossRef]
12. Takasu, A.; Ito, M.; Inai, Y.; Hirabayashi, T.; Nishimura, Y. Synthesis of biodegradable polyesters by ring-opening copolymerization of cyclic anhydrides containing a double bond with 1,2-epoxybutane and one-pot preparation of the itaconic acid-based polymeric network. *Polym. J.* **1999**, *31*, 961–969. [CrossRef]
13. Tang, T.; Moyori, T.; Takasu, A. Isomerization-free polycondensations of cyclic anhydrides with diols and preparation of polyester gels containing cis or trans carbon double bonds via photo-cross-linking and isomerization in the gels. *Macromolecules* **2013**, *46*, 5464–5472. [CrossRef]
14. Farmer, T.; Castle, R.; Clark, J.; Macquarrie, D. Synthesis of unsaturated polyester resins from various bio-derived platform molecules. *Int. J. Mol. Sci.* **2015**, *16*, 14912–14932. [CrossRef] [PubMed]
15. Winkler, M.; Lacerda, T.M.; Mack, F.; Meier, M.A.R. Renewable polymers from itaconic acid by polycondensation and ring-opening-metathesis polymerization. *Macromolecules* **2015**, *48*, 1398–1403. [CrossRef]
16. Bai, Y.; De bruyn, M.; Clark, J.H.; Dodson, J.R.; Farmer, T.J.; Honore, M.; Ingram, I.D.V.; Naguib, M.; Whitwood, A.C.; North, M. Ring opening metathesis polymerization of a new bio-derived monomer from itaconic anhydride and furfuryl alcohol. *Green Chem.* **2016**, *18*, 3945–3948. [CrossRef]
17. Lv, A.; Li, Z.-L.; Du, F.-S.; Li, Z.-C. Synthesis, functionalization, and controlled degradation of high molecular weight polyester from itaconic acid via ADMET polymerization. *Macromolecules* **2014**, *47*, 7707–7716. [CrossRef]
18. Nagai, S.; Yoshida, K. Polymerization of itaconic acid derivatives. Part III: Rate of polymerization of dialkyl itaconates. *Kobunshi Kagaku* **1960**, *17*, 79–82. [CrossRef]
19. Braun, V.D.; Ahn, T.-O. Copolymerisation von Itaconsauredialkylestern mit Styrol. *Kolloid Z.* **1963**, *188*, 1–4. [CrossRef]
20. Sato, T.; Morita, N.; Tanaka, H.; Ota, T. Solvent effect on the radical polymerization of di-n-butyl itaconate. *J. Polym. Sci. A Polym. Chem.* **1989**, *27*, 2497–2508. [CrossRef]
21. Otsu, T.; Watanabe, H. Radical polymerization reactivity of dialkyl itaconates and characterization of their polymers. *Eur. Polym. J.* **1993**, *29*, 167–174. [CrossRef]
22. Fernandez-Garcia, M.; Madruga, E.L. Glass transition in dimethyl and di-n-butyl poly(itaconate ester)s and their copolymers with methyl methacrylate. *Polymer* **1997**, *38*, 1367–1371. [CrossRef]
23. Madruga, E.L.; Fernandez-Garcia, M. Free-radical homopolymerization and copolymerization of di-n-butyl itaconate. *Polymer* **1994**, *35*, 4437–4442. [CrossRef]
24. Veličković, J.; Filipović, J.; Djakov, D.P. The synthesis and characterization of poly(itaconic) acid. *Polym. Bull.* **1994**, *32*, 169–172. [CrossRef]

25. Hirano, T.; Takeyoshi, R.; Seno, M.; Sato, T. Chain-transfer reaction in the radical polymerization of di-n-butyl itaconate at high temperatures. *J. Polym. Sci. A Polym. Chem.* **2002**, *40*, 2415–2426. [\[CrossRef\]](#)
26. Hirano, T.; Higashi, K.; Seno, M.; Sato, T. Radical polymerization of di-n-butyl itaconate in the presence of Lewis acids. *Eur. Polym. J.* **2003**, *39*, 1801–1808. [\[CrossRef\]](#)
27. Hirano, T.; Higashi, K.; Seno, M.; Sato, T. Reaction control in radical polymerization of di-n-butyl itaconate utilizing a hydrogen-bonding interaction. *J. Polym. Sci. A Polym. Chem.* **2004**, *42*, 4895–4905. [\[CrossRef\]](#)
28. Rangel-Rangel, E.; Torres, C.; Rincon, L.; Loteich-Khatib, S.; Lopez-Carrasquero, F. Copolymerizations of long side chain di n-alkyl itaconates and methyl n-alkyl itaconates with styrene: Determination of monomers reactivity ratios by NMR. *Rev. Latinoam. Metal. Mater.* **2012**, *32*, 79–88.
29. Lopez-Carrasquero, F.; Rangel-Rangel, E.; Cardenas, M.; Torres, C.; Dugarte, N.; Laredo, E. Copolymers of long-side-chain di-n-alkyl itaconates or methyl m-alkyl itaconates with styrene: Synthesis, characterization, and thermal properties. *Polym. Bull.* **2013**, *70*, 131–146. [\[CrossRef\]](#)
30. Sarkar, P.; Bhowmick, A.K. Green approach toward sustainable polymer: Synthesis and characterization of poly(myrcene-co-dibutyl itaconate). *ACS Sustain. Chem. Eng.* **2016**, *4*, 2129–2141. [\[CrossRef\]](#)
31. Lei, W.; Russell, T.P.; Hu, L.; Zhou, X.; Qiao, H.; Wang, W.; Wang, R.; Zhang, L. Pendant Chain effect on the synthesis, characterization, and structure–property relations of poly (di-n-alkyl itaconate-co-isoprene) biobased elastomers. *ACS Sustain. Chem. Eng.* **2017**, *5*, 5214–5223. [\[CrossRef\]](#)
32. Szablan, Z.; Toy, A.A.; Terrenoire, A.; Davis, T.P.; Stenzel, M.H.; Müller, A.H.E.; Barner-Kowollik, C. Living free-radical polymerization of sterically hindered monomers: Improving the understanding of 1,1 di-substituted monomer systems. *J. Polym. Sci. A Polym. Chem.* **2006**, *44*, 3692–3710. [\[CrossRef\]](#)
33. Satoh, K.; Lee, D.-H.; Nagai, K.; Kamigaito, M. Precision Synthesis of Bio-Based Acrylic Thermoplastic Elastomer by RAFT Polymerization of Itaconic Acid Derivatives. *Macromol. Rapid Commun.* **2014**, *35*, 161–167. [\[CrossRef\]](#) [\[PubMed\]](#)
34. Fernandez-Garcia, M.; Fernandez-Sanz, M.; De la Fuente, J.L.; Madruga, E.L. Atom-transfer radical polymerization of dimethyl itaconate. *Macromol. Chem. Phys.* **2001**, *202*, 1213–1218. [\[CrossRef\]](#)
35. Okada, S.; Matyjaszewski, K. Synthesis of bio-based poly(N-phenylitaconimide) by atom transfer radical polymerization. *J. Polym. Sci. A Polym. Chem.* **2015**, *53*, 822–827. [\[CrossRef\]](#)
36. Inciarte, H.; Orozco, M.; Fuenmayor, M.; López-Carrasquero, F.; Oliva, H. Comb-like copolymers of n-alkyl monoitaconates and styrene. *e-Polymers* **2006**, *6*. [\[CrossRef\]](#)
37. Nagai, S. The polymerization and polymers of itaconic acid derivatives. VI. The polymerization and copolymerization of itaconic anhydride. *Bull. Chem. Soc. Jpn.* **1964**, *37*, 369–373. [\[CrossRef\]](#)
38. Wallach, J.A.; Huang, S.J. Copolymers of itaconic anhydride and methacrylate-terminated poly(lactic acid) macromonomers. *Biomacromolecules* **2000**, *1*, 174–179. [\[CrossRef\]](#)
39. Shang, S.; Huang, S.J.; Weiss, R.A. Synthesis and characterization of itaconic anhydride and stearyl methacrylate copolymers. *Polymer* **2009**, *50*, 3119–3127. [\[CrossRef\]](#)
40. Javakhishvili, I.; Kasama, T.; Jankova, K.; Hvilsted, S. RAFT copolymerization of itaconic anhydride and 2-methoxyethyl acrylate: A multi-functional scaffold for preparation of “clickable” gold nanoparticles. *Chem. Commun.* **2013**, *49*, 4803–4805. [\[CrossRef\]](#)
41. Nicolas, J.; Guillaneuf, Y.; Lefay, C.; Bertin, D.; Gigmes, D.; Charleux, B. Nitroxide mediated polymerization. *Prog. Polym. Sci.* **2013**, *38*, 63–235. [\[CrossRef\]](#)
42. Willcock, H.; O'Reilly, R.K. End group removal and modification of RAFT polymers. *Polym. Chem.* **2010**, *1*, 149–157. [\[CrossRef\]](#)
43. Su, X.; Jessop, P.G.; Cunningham, M.F. ATRP catalyst removal and ligand recycling using CO₂-switchable materials. *Macromolecules* **2018**, *51*, 8156–8164. [\[CrossRef\]](#)
44. Wang, Y.; Lorandi, F.; Fantin, M.; Chmielarz, P.; Isse, A.A.; Gennaro, A.; Matyjaszewski, K. Miniemulsion ARGET ATRP via interfacial and ion-pair catalysis: From ppm to ppb of residual copper. *Macromolecules* **2017**, *50*, 8417–8425. [\[CrossRef\]](#)
45. Vinas, J.; Chagneux, N.; Gigmes, D.; Trimaille, T.; Favier, A.; Bertin, D. SG1-based alkoxyamine bearing a N-succinimidyl ester: A versatile tool for advanced polymer synthesis. *Polymer* **2008**, *49*, 3639–3647. [\[CrossRef\]](#)
46. Szablan, Z.; Stenzel, M.H.; Davis, T.P.; Barner, L.; Barner-Kowollik, C. Depropagation kinetics of sterically demanding monomers: A pulsed laser size exclusion chromatography study. *Macromolecules* **2005**, *38*, 5944–5954. [\[CrossRef\]](#)

47. Buback, M.; Gilbert, R.G.; Hutchinson, R.A.; Klumperman, B.; Kuchta, F.D.; Manders, B.G.; O'Driscoll, K.F.; Russell, G.T.; Schweer, J. Critically evaluated rate coefficients for free-radical polymerization, 1. Propagation rate coefficient for styrene. *Macromol. Chem. Phys.* **1995**, *196*, 3267–3280. [\[CrossRef\]](#)
48. Kassi, E.; Loizou, E.; Porcar, L.; Patrickios, C.S. Di(n-butyl) itaconate end-functionalized polymers: Synthesis by group transfer polymerization and solution characterization. *Eur. Polym. J.* **2011**, *47*, 816–822. [\[CrossRef\]](#)
49. Kassi, E.; Constantinou, M.S.; Patrickios, C.S. Group transfer polymerization of bio-based monomers. *Eur. Polym. J.* **2013**, *49*, 761–767. [\[CrossRef\]](#)
50. Tomić, S.L.; Filipović, J.M.; Velicković, J.S.; Katsikas, L.; Popović, I.G. The polymerisation kinetics of lower dialkyl itaconates. *Macromol. Chem. Phys.* **1999**, *200*, 2421–2427. [\[CrossRef\]](#)
51. Benoit, D.; Grimaldi, S.; Robin, S.; Finet, J.P.; Tordo, P.; Gnanou, Y. Kinetics and mechanism of controlled free-radical polymerization of styrene and n-butyl acrylate in the presence of an acyclic-phosphonylated nitroxide. *J. Am. Chem. Soc.* **2000**, *122*, 5929–5939. [\[CrossRef\]](#)
52. Fukuda, T.; Ma, Y.-D.; Inagaki, H. Free radical copolymerization. 3. Determination of rate constants of propagation and termination for styrene/methyl methacrylate system. A critical test of terminal-model kinetics. *Macromolecules* **1985**, *18*, 17–26. [\[CrossRef\]](#)
53. Fischer, H. The persistent radical effect in controlled radical polymerizations. *J. Polym. Sci. A Polym. Chem.* **1999**, *37*, 1885–1901. [\[CrossRef\]](#)
54. Charleux, B.; Nicolas, J.; Guerret, O. Theoretical expression of the average activation-deactivation equilibrium constant in controlled/living free-radical copolymerization operating via reversible termination. Application to a strongly improved control in nitroxide-mediated polymerization of methyl methacrylate. *Macromolecules* **2005**, *38*, 5484–5492.
55. Ma, Y.D.; Sung, K.S.; Tsujii, Y.; Fukuda, T. Free-radical copolymerization of styrene and diethyl fumarate. Penultimate-unit effects on both propagation and termination processes. *Macromolecules* **2001**, *34*, 4749–4756. [\[CrossRef\]](#)
56. Lessard, B.; Marić, M. Effect of acrylic acid neutralization on 'livingness' of poly[styrene-ran-(acrylic acid)] macro-initiators for nitroxide-mediated polymerization of styrene. *Polym. Int.* **2008**, *57*, 1141–1151. [\[CrossRef\]](#)
57. Buback, M.; Egorov, M.; Junkers, T.; Panchenko, E. Termination kinetics of dibutyl itaconate free-radical polymerization studied via the SP–PLP–ESR technique. *Macromol. Chem. Phys.* **2005**, *206*, 333–341. [\[CrossRef\]](#)
58. Buback, M.; Kuchta, F.D. Termination kinetics of free-radical polymerization of styrene over an extended temperature and pressure range. *Macromol. Chem. Phys.* **1997**, *198*, 1455–1480. [\[CrossRef\]](#)
59. Yee, L.H.; Heuts, J.A.P.; Davis, T.P. Copolymerization propagation kinetics of dimethyl itaconate and styrene: Strong entropic contributions to the penultimate unit effect. *Macromolecules* **2001**, *34*, 3581–3586. [\[CrossRef\]](#)
60. Szablan, Z.; Toy, A.A.; Davis, T.P.; Hao, X.; Stenzel, M.H.; Barner-Kowollik, C. Reversible addition fragmentation chain transfer polymerization of sterically hindered monomers: Toward well-defined rod/coil architectures. *J. Polym. Sci. A Polym. Chem.* **2004**, *42*, 2432–2443. [\[CrossRef\]](#)
61. Marque, S.; Le Mercier, C.; Tordo, P.; Fischer, H. Factors influencing the C–O–bond homolysis of trialkylhydroxylamines. *Macromolecules* **2000**, *33*, 4403–4410. [\[CrossRef\]](#)
62. Veličković, J.; Čoseva, S.; Fort, R.J. Solution properties of poly(dicyclohexyl itaconate). *Eur. Polym. J.* **1975**, *11*, 377–380. [\[CrossRef\]](#)
63. Strazielle, C.; Benoit, H.; Vogl, O. Preparation et caractérisation des polymères tête-à-tête—VI: Propriétés physicochimiques du polystyrène tête-à-tête en solution diluée. Comparaison avec des polystyrènes de structure différente. *Eur. Polym. J.* **1978**, *14*, 331–334. [\[CrossRef\]](#)
64. Andrews, R.J.; Grulke, E.A. Glass transition temperatures of polymers. In *Polymer Handbook*, 4th ed.; Brandrup, J., Immergut, E.H., Grulke, E.A., Abe, A., Bloch, D.R., Eds.; Wiley: New York, NY, USA, 1999; Volume 1, pp. 181–308.
65. Arrighi, V.; Holmes, P.F.; McEwen, I.J.; Qian, H.; Terrill, N.J. Order in amorphous di-n-alkyl itaconate polymers, copolymers, and blends. *J. Polym. Sci. B Polym. Phys.* **2004**, *42*, 4000–4016. [\[CrossRef\]](#)
66. Cowie, J.M.G. Physical properties of polymers based on itaconic acid. *Pure Appl. Chem.* **1979**, *51*, 2331–2343. [\[CrossRef\]](#)

